Available online at www.sciencedirect.com
ScienceDirect
Renewable and Sustainable Energy Reviews
12 (2008) 2040–2065

RENEWABLE
& SUSTAINABLE
ENERGY REVIEWS

www.elsevier.com/locate/rser

Short-term prediction of household electricity consumption: Assessing weather sensitivity in a Mediterranean area

M. Beccali, M. Cellura, V. Lo Brano, A. Marvuglia*

Dipartimento di Ricerche Energetiche ed Ambientali (DREAM), Università degli Studi di Palermo, Viale delle Scienze, 90128 Palermo, Italy

Received 29 March 2007; accepted 16 April 2007

Abstract

Urban microclimatic variations, along with a rapid reduction of unit cost of air-conditioning (AC) equipments, can be addressed as some of the main causes of the raising residential energy demand in the more developed countries. This paper presents a forecasting model based on an Elman artificial neural network (ANN) for the short-time prediction of the household electricity consumption related to a suburban area. Due to the lack of information about the real penetration of electric appliances in the investigated area and their utilization profiles it was not possible to implement a statistical model to define the weather and climate sensitivities of appliance energy consumption. For this reason an ANN model was used to predict the household electric energy demand of the investigated area and to evaluate the influence of the AC equipments on the overall consumption.

The data used to train the network were recorded in Palermo (Italy) and include electric current intensity and weather variables as temperature, relative humidity, global solar radiation, atmospheric pressure and wind speed values between June 1, 2002 and September 10, 2003.

The work pointed out the importance of a thermal discomfort index, the *Humidex index*, for a simple but effective evaluation of the conditions affecting the occupant behaviour and thus influencing the household electricity consumption related to the use of heating, ventilation and air conditioning (HVAC) appliances. The prediction performances of the model are satisfying and bear

*Corresponding author. Tel.: +39 091236118; fax: +39 091484425.
E-mail address: marvuglia@dream.unipa.it (A. Marvuglia).

doi:10.1016/j.rser.2007.04.010

out the ability of ANNs to manage incomplete and noisy data, solve nonlinear problems and learn complex underlying relationships between input and output patterns.

Keywords: Short-term load forecasting; HVAC; Household electricity consumption; ANN; Elman neural network

Contents

1. Introduction

Over the last decade the electric energy consumption in the residential sector has significantly increased especially in the summer season, because of the increasing use of air-conditioning (AC) systems, that has drastically changed the thermal comfort needs of urban population in the developed countries. The strong penetration of the AC equipments on the market was also quickened by the sudden and rapid reduction of their cost along with the significant temperature rise in densely built urban areas with respect to the surrounding areas, known as "urban heat island" effect [1,2]. The particular microclimatic conditions of the urban areas have in fact a significant influence on the thermal balance of the buildings.

In the paper one shows a forecasting model for the household electric consumption of a particular area within a district of the town of Palermo (Italy).

The forecasting model is based on an Elman recurrent neural network (RNN) [3]. Several Elman networks were tested and the best model was sought in order to obtain the lowest prediction error rates and to assess the influence of AC systems on the electric energy consumption of the investigated area. The model estimates the electricity consumption for each hour of the day, starting from weather data and electricity demand related to the hour before the hour of the forecast. It also takes into account other variables which will be better described in the following sections.

The original contribution of the work lies in the exploitation of a comfort index (the *Humidex index*) within a neural network (NN) model for the evaluation of the influence of the AC equipments on the overall residential consumption of the studied area. The utilization of a NN model is justified by the presence of inaccurate data concerning the presence of the heating, ventilation and air conditioning (HVAC) function equipments.

The sensitivity analysis accomplished in the last part of the paper gives an explanatory insight into the relative influence of the variables selected as independent variables in the prediction process.

1.1. Factors affecting the residential electricity consumption and methods for energy and load estimations

Electricity demand depends on economic variables and national circumstances as well as on climatic conditions. In the most of the electricity systems the residential sector is one of the main contributors to the load peaks [4]. In the residential sector, the energy consumption depends on the features of the building envelope and on the occupant behaviour as well. The latter is subject to many factors including householders' subjective comfort preferences and their socio-demographic and socio-economic characteristics [5]. On the other hand, it is well known that "awareness and attitudes toward energy consumption are more evident in household consumption than in situations where many people may simultaneously have an influence on energy use, such as in office buildings" [6].

In addition to the multiplicity of human factors affecting the energy demand, numerous studies have illustrated the influence of weather variables on energy consumption and especially on electricity demand. The approaches so far employed for load forecasting include statistical/regression models [7] or econometric models [8], engineering models [9], structural models [10], fuzzy logic and expert systems [11].

The engineering models are based on a vast amount of equations by which the energy end-use estimation is accomplished starting from a detailed engineering knowledge about technical and constructional features of different houses as well as behavioural information, e.g. about use and power need of household electric appliances. According to Bartels and Fiebig [12] "Engineering models are only appropriate, however, in situations where individual behaviour plays a minor rule, for example, heating and cooling in extreme climates. Most appliance use depends on the life style; in temperate climates, even heating and cooling appliances are, in many households, only used when the occupants are at home." Furthermore, being them based upon theoretical considerations, rather than observed consumer behaviour, they are not enough flexible with respect to changes in price, incomes, or household sizes. Among the econometric approaches the most widespread in the scientific literature is the conditional demand analysis (CDA), first employed by Parti and Parti [13]. The CDA model estimates mean electricity consumption for each household electric appliance and multiplies it by the shares of households possessing the appliances, in order to give estimates of mean electricity consumption for different appliances for the average household. An advantage of the econometric CDA model, is that end-use parameters are estimated directly, without having to make assumptions regarding behaviour and technicalities, but the number of buildings in the data base has to be large because of the regression analysis.

For single buildings it is common to use load and energy simulation programs, which model the energy balances in the buildings including transmission, ventilation and infiltration losses.

For time series prediction problems the use of NNs is also very common [14]. For this task different approaches have been used, based for example on the application of self-organizing maps (SOMs), recurrent SOMs, multi-layer perceptrons (MLPs), or a combination of SOMs and MLPs [15]. Specific studies based on the application of NNs have been successfully carried out to predict the residential end-use energy consumption [16]. In a NN the relation between inputs and outputs is driven from the data themselves, through a process of training that consists in the modification of the weights associated to the connections, utilizing specific algorithms called *learning algorithms*.

NNs are particularly suited for load and energy estimations and whenever the data to be processed have some missing or incomplete values, as often happens with metered energy or weather data. NN-based models are also able to solve nonlinear problems and "exhibit robustness and fault tolerance" [17].

1.2. Growing AC demand in the urban environment

In 2004 the final energy consumption in households in the European Union (EU-25) approached 300 Mtoe, which represents about 26.9% of the total energy consumption. This means that the household sector is responsible for about 12.2% of the total CO_2 emissions [18].

Although in many countries the primary energy consumption for heating is being reduced because of the effective energy conservation measures adopted, in Southern Europe, and recently also in Central and Northern Europe, the primary energy consumption continues to increase, mainly due to the propagation of AC appliances.

In fact, especially in the Mediterranean countries, peaks in the electricity demand occur more frequently during the summer period than during the winter. This growing demand is being strengthened by the urban heat island effect, which results in higher air temperatures in densely built towns, thus enhancing the cooling load in commercial and residential buildings [19].

In the meantime, the extended use of air-conditioners, mainly of split-unit devices, increases the heat island in densely built urban areas. The heat rejected by the compressor units contributes to warm up the outdoor air in the narrow streets, thus increasing even more the cooling demand of the buildings and further reducing the coefficient of performance (COP) of the air-conditioners. All this creates a vicious circle in terms of cooling and power demand [20].

On the other hand, room air-conditioners sales drastically increased. The Italian market for air-conditioners has been increasing since 2002. Up to 2003 it was the largest in Europe, accounting for 25% of the total European market [21]. Italian production accounts for an even larger share, of approximately 30% of total EU production. The survey includes 70–75% of the total residential split systems market. According to the statistics for 2004 in the single-split and multi-split air-conditioners sales heat pumps accounts for more than 67% of the units, and inverter driven compressors are nearly 33% of the units. For the same category of appliances, the growth from 2003 to 2004 was estimated around 42.6%, while from 2002 to 2003 (a year characterized by a particularly hot summer) the sales' rise percentage had been 46.2% [22].

The market is steadily growing for residential, light commercial and central AC (mostly chillers) systems. Looking at the reports published by the Italian National Grid Operator (GRTN—Gestore della Rete di Trasmissione Nazionale) one observes that the summer peak loads are now higher than the winter ones. As an example, the peak load of 2005 summer (54,163 MW) exceeded the one of 2004 summer by 600 MW. It was also higher than the last winter consumption record (53,600 MW, December, 16th, 2004). According to the annual reports published by GRTN, the Italian summer peak load during the years 2000–2005 showed a rise of 25% or 8.38 GW [23].

The change is also showed by the daily maximum demand curves, as monitored in July and August 2000, 2003 and 2005 (see Fig. 1). Table 1 shows the trend of the Italian household electricity consumption in the years from 2000 to 2004.

Moreover, in recent years the Italian national power company coped with several blackout situations occurred during very hot summer days. The coincidence between

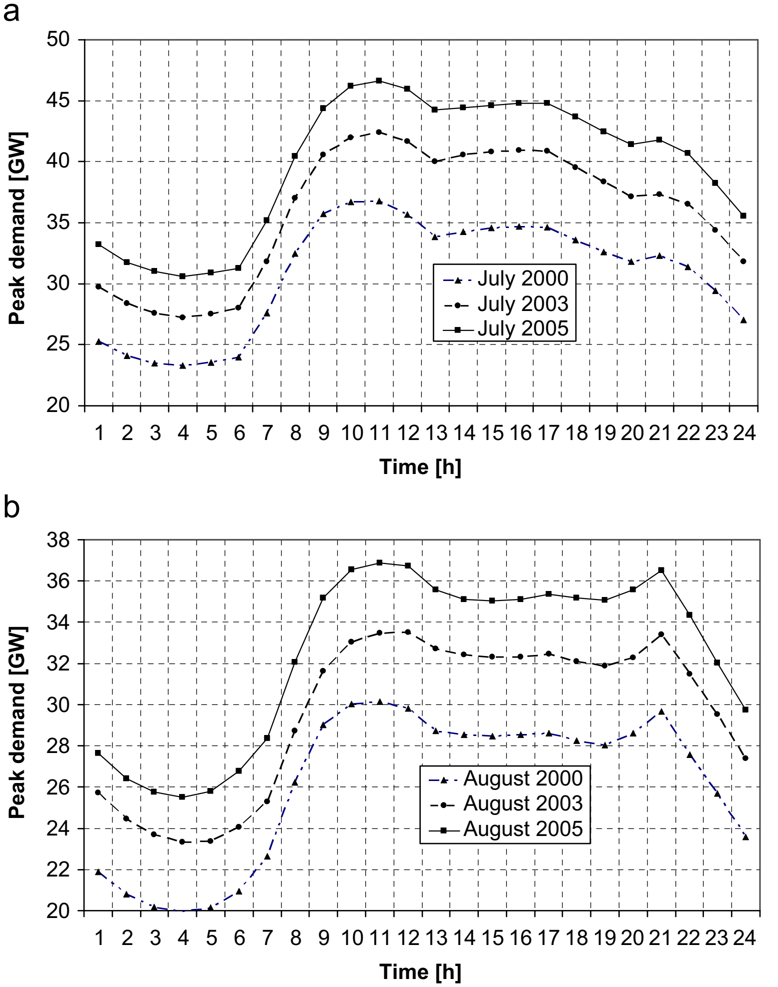


Fig. 1. Evolution of the daily peak load profile in Italy for the months of: (a) July and (b) August.

Table 1
Italian total electric energy consumption in residential buildings from 2000 to 2004

Year	2000	2001	2002	2003	2004
Household electricity demand (GW h)	61.1	61.6	63.0	65.0	66.6

Source: [23].

overload conditions for the power grid and peak values for air humidity and temperature makes one suppose an high correlation between use of cooling appliances and electric energy demand. Starting from these remarks, it is possible to understand the importance, for private and public power corporations, of reliable short and very short-term load forecasting (STLF) models. A very precise forecast allows the producer to identify in advance any emergency situation and to tackle it by quick adjustments of local energy dispatchment or suitable scheduling of plants start up/shut down operations.

2. Short description of the work

The Elman NN presented in this paper is able to predict the electric current intensity (C) at time t, knowing the values of several variables at time $(t-1)$. The work started with the collection of different types of data:

1. climatic data (i.e. hourly average values of temperature T, relative air humidity RH, global solar radiation R, atmospheric pressure P, wind speed W);
2. time series of the hourly average values of electric current intensity withdrawn by the users connected to a small grid in the area of Palermo;
3. a variable (*HS index*) related to the estimated number of the residential air-conditioners utilized within the investigated area;
4. a variable, named *Humidex index* (H), linked to T and RH, whose aim is to quantify the discomfort level perceived by the occupants of the dwellings.

The electric consumption data have been split by GRTN according to the different use destination (household, industrial and commercial sector) and, in view of the aims of this study, only the data regarding the residential sector have been used for the network's training.

Weather data, electric current intensity and *HS index* at time $(t-1)$ represent the inputs of the model; current intensity at time t represents its output.

Several trainings have been carried out by using different type of Elman networks, varying the number of hidden neurons and the parameters of the training algorithm. Finally, a sensitivity analysis was accomplished on the input variables in order to evaluate the importance of each of them on the output of the network. A MLP was also used to tackle the same problem and the performances of the two models were compared.

3. The Elman NN

Elman NNs [3] are also known as partially recurrent networks or simple recurrent networks. These are MLP networks augmented with an additional *context layer* which

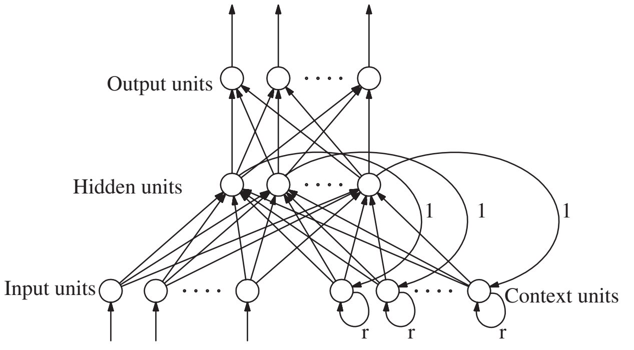


Fig. 2. Schematic representation of an Elman recurrent neural network.

store the output values of the hidden layer delayed by one step. The network has feedback from each of the hidden units to all of the hidden units, as shown in Fig. 2. Each context unit has an auto-connection with a constant weight r, called *recency constant*. Useful values of r are between 0 and 1. A value of 1 means that all the past is factored in. On the other extreme, a value equal to 0 means that only the present time is factored in (i.e., there is no self-recurrent connection). The closer the value is to 1, the longer the memory depth and the slower the forgetting factor.

The feedback from the hidden to the context layer allows Elman networks to learn, recognize and generate temporal patterns, as well as spatial patterns. Every hidden neuron is connected to only one neuron of the context layer through a constant weight equal to +1. Hence, the context layer constitutes a kind of copy of the state of the hidden layer, one instant before. The number of context neurons is consequently the same as the number of hidden neurons.

The output vector of an Elman network is computed as

$$\mathbf{O}(t+1) = \mathbf{C}^T\mathbf{z}(t) + \mathbf{c}_0, \tag{1}$$

and

$$\mathbf{z}(t) = F_{n_\mathrm{h}}(\mathbf{A}\mathbf{k}(t) + \mathbf{B}^T\mathbf{u}(t) + \mathbf{b}), \tag{2}$$

where $\mathbf{O}(t+1)$ is $n_\mathrm{o} \times 1$ vector (being n_o the number of output units) containing the outputs of the network; $\mathbf{C}$ is a $n_\mathrm{h} \times n_\mathrm{o}$ matrix (being n_h the number of hidden units and n_o the number of output units) which represents the weights from the hidden layer to the output units; $\mathbf{c}_0$ is a constant bias vector; $\mathbf{z}(t) \in \Re^{n_\mathrm{h}}$ is an $n_\mathrm{h} \times 1$ vector denoting the outputs of the hidden units at the time step t; $\mathbf{A}$ is a $n_\mathrm{c} \times n_\mathrm{h}$ matrix (being $n_\mathrm{c} = n_\mathrm{h}$ the number of context layer units) which represents the weights from the context units to the hidden units; $\mathbf{k}(t)$ is a $n_\mathrm{c} \times 1$ vector denoting the output of the context units (see Eq. (15)); $\mathbf{B}$ is a $n_\mathrm{i} \times n_\mathrm{h}$ matrix (being n_i the number of inputs) which represents the weights from the input layer to the hidden layer; $\mathbf{b}$ is a $n_\mathrm{h} \times 1$ vector containing the *bias* values of the hidden units; $\mathbf{u}(t)$ is the input vector, whose dimension is $n_\mathrm{i} = d_\mathrm{e} \times 1$ (being d_e the so-called *embedding dimension*, that is the number of past input values used to compute the next

value of the time series):

$$\mathbf{u}(t) = \begin{bmatrix} s(t) \\ s(t-1) \\ \vdots \\ s(t-d_e+1) \end{bmatrix}. \quad (3)$$

F_{n_h} is an $n_h \times 1$ vector containing the activation functions of the hidden units.

In Eq. (3), $s(t)$ is the input variable (or the vector of input variables) sampled at time t.

3.1. Learning procedures

The primary aim of developing an artificial neural network (ANN) for time series analysis is to generalize the features of the processed time series. Unfortunately, it is not obvious what size of the network is the best to achieve this task. A network that is not sufficiently complex is very sensitive to initial conditions and can fail to fully detect the signal in a complicated data set, leading to *underfitting*. On the other hand, larger networks have more functional flexibility than small networks so are better able to fit the data, but if the network has too many weights it may fit the noise and not just the signal, thus leading to *overfitting* [24]. Overfitting produces excessive variance and can also produce rough predictions in MLPs even with noise-free data; whereas underfitting produces excessive bias in the output. A popular technique to achieve generalization, avoiding overfitting, is the *early stopping* method presented by Sarle [25]. According to this method, the generated data set has to be divided into three subsets: a *training set*, a *validation set*, and a *test set*. A training set is a portion of a data set used to train a NN for prediction or classification purposes. The error on the validation set is monitored during the training process. The validation error will normally decrease during the initial phase of training, as does the training set error. However, when the network begins to overfit the data, the error on the validation set will typically begin to rise. When the validation error increases for a specified number of iterations, the training is stopped, and the weights and biases at the minimum of the validation error are returned. The test set error is not used during the training, but it is used as a more objective measure of the performance of various models that have been fitted to the training data.

4. The case-study: a small residential area in the town of Palermo

In this section the studied area and the data warehouse are described. Furthermore, the model selection process is explained and an example of its forecasting performances is showed. In order to select the best network architecture and training parameters, several models were trained and tested. The main outcomes of this design process and the final obtained results are described in the following sections.

4.1. The data warehouse

As previously stated, the present study deals with the electric energy consumption of a small district of the town of Palermo. The climate of Palermo is typically

Mediterranean, mild and humid because of the vicinity of the sea. In Fig. 3(a) the position of the town of Palermo within Sicily is showed and in Fig. 3(b) the investigated area is highlighted.

The data used as input of the model can be divided into measured data (electric current intensity and weather data) and data calculated starting from the measured data (*HS index*, *Humidex index*).

The time series of the electric current intensity is constituted by the hourly mean values collected in the period from June, 1st, 2002 to September, 10th 2003. The series is not complete because the data related to several hours are missing. These data were supplied by GRTN; the weather data were supplied by the Astronomic Observatory G. Vajana of Palermo. It is apparent that the household electricity consumption is strongly influenced by the utilization of household appliances. In particular, one of the aim of the present study is the estimation of the influence of the use of AC appliances on the overall domestic electricity demand.

The number of AC devices in the investigated area was assessed by using statistical data and inspection data. More in detail, statistical data concerning the trend of AC appliances sales in Italy in years 2002 and 2003 [22] were used; then this trend was linked to the number of appliances surveyed in the studied area through a visual inspection accomplished in 2003 (see Table 2).

The data on a local scale for the whole period June 2002–September 2003 were obtained by assuming the same yearly percentage variation as the national data. By this link it was possible to estimate the temporal trend of the number of air-conditioners installed in the suburban area in question.



Fig. 3. (a) Position of the town of Palermo within Sicily region; and (b) air view of a part of Palermo and localization of the investigated area.

Table 2
Number of air-conditioning devices observed in the investigated district during the survey of 2003 and number of split and multi-split AC systems sold in Italy in 2002 and 2003

Year	2002	2003	Δ% 2003/2002
Number of AC devices surveyed in the studied area	–	375	46.2
Split and multi-split AC appliances sold in Italy	924,887	1,352,070	

Source: [22].

The effect of changes in weather conditions on electricity load can be significant. Even if the available data set is not very wide, with a simple plot it is possible to observe that the variation of electricity demand with temperature is not linear. In Fig. 4 it is showed the trend of the electricity demand as a function of the daily mean temperature for the same period. By finding the minimum point of the quadratic regression curve it is possible to state that at approximately 18.7 °C the influence of the temperature is minimized and the electricity demand is inelastic to temperature changes.

In Fig. 5 the electricity demand is split into a "summer" (including months from June to September) and "winter" one (the remaining months of the year) and the corresponding regression curves are showed together with their equations and the value of the coefficient of determination R^2. Especially for the cooling period the outdoor temperature bears a close relationship to the electricity consumption ($R^2 = 0.7$). A method which is universally used in the HVAC industry to relate the outdoor air temperature to the energy consumption is based on the concept of degree-days and, on a finer temporal scale, degree hours. The methods based on the concept of degree-days assume that the energy needs for a specific building in a specific location are proportional to the difference between the daily mean temperature and a base temperature. The base temperature is the outdoor temperature below or above which heating or cooling are needed [26].

The heating degree-days (HDD_t) and the cooling degree-days (CDD_t) of the day t can be estimated on the basis of the following equations:

$$HDD_t = \max(T_{ref} - T_t; 0), \tag{4}$$

$$CDD_t = \min(T_{ref} - T_t; 0), \tag{5}$$

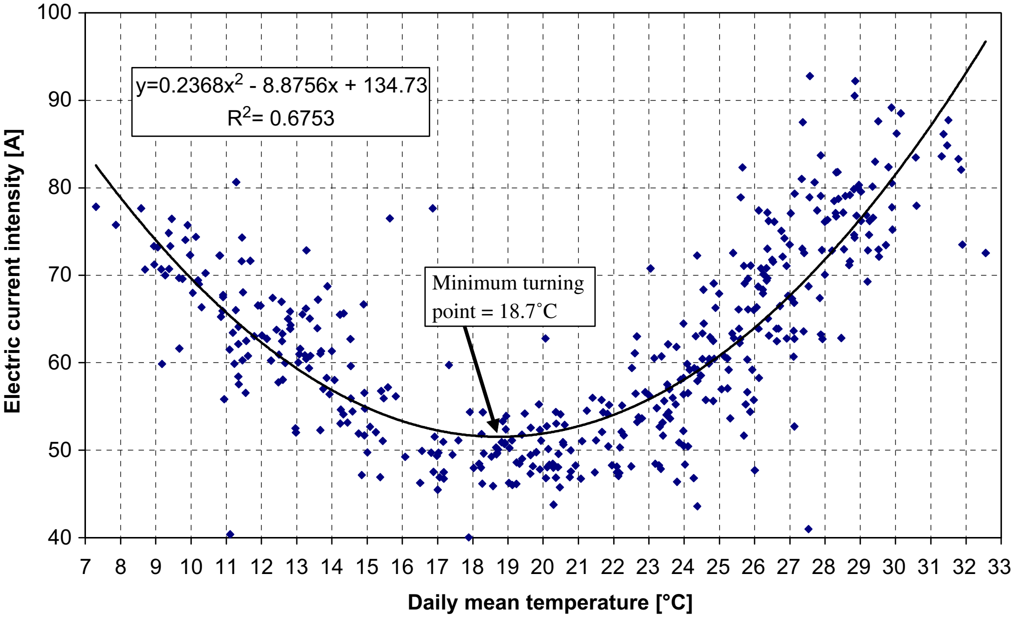


Fig. 4. Relationship between electricity demand and temperature for the investigated district.

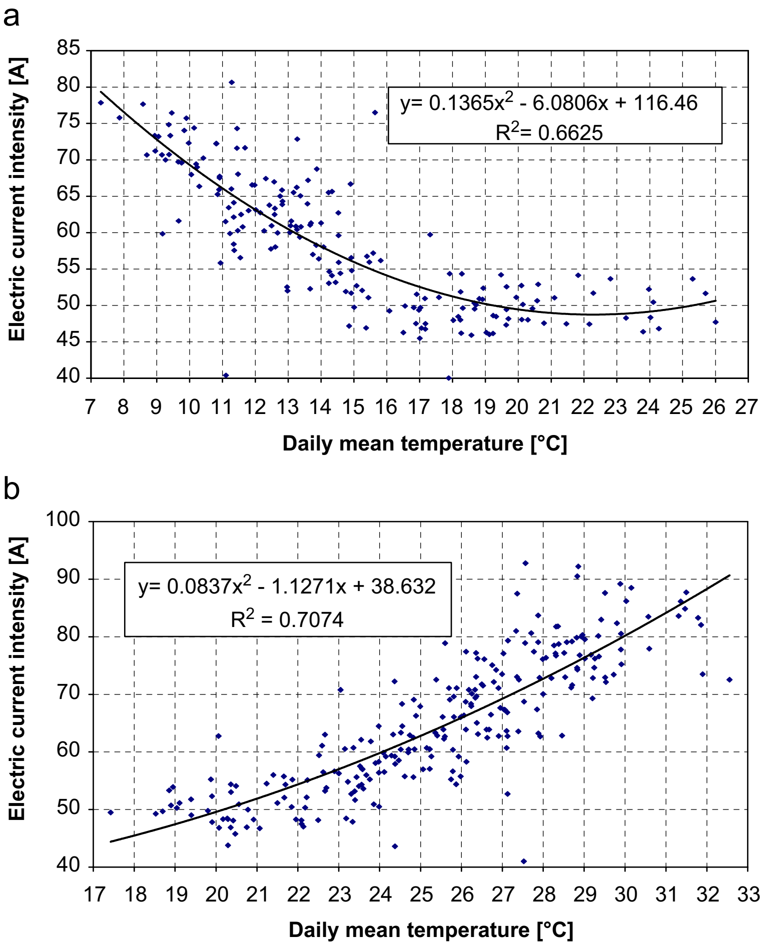


Fig. 5. Relationship between electricity demand and temperature for: (a) the heating season; and (b) the cooling season.

where T_t is the average temperature for the day t; T_{ref} is a reference temperature that should be adequately selected to separate the heat and cold branches of the demand–temperature relationship; it is generally regarded as the outdoor temperature at which neither artificial heating nor cooling is required.

Traditionally, HDD are calculated at a base temperature of 18 °C, whilst for CDD the base temperature is not so unanimously agreed. A common value for it, in typical non-insulated buildings, is 22 °C [27]. However, the average value of T_{ref} varies widely from one building to another, because of significant differences in the personal comfort preferences of the occupants and because of different building characteristics such as thermal insulation, ventilation rates and solar gains. Hence degree-days with a base temperature of 18 °C in heating or 22 °C in cooling must be employed with caution. However, as the building types and the ventilation rates were not known for the dwellings located within the investigated area, in the present study the CDD were calculated using a base

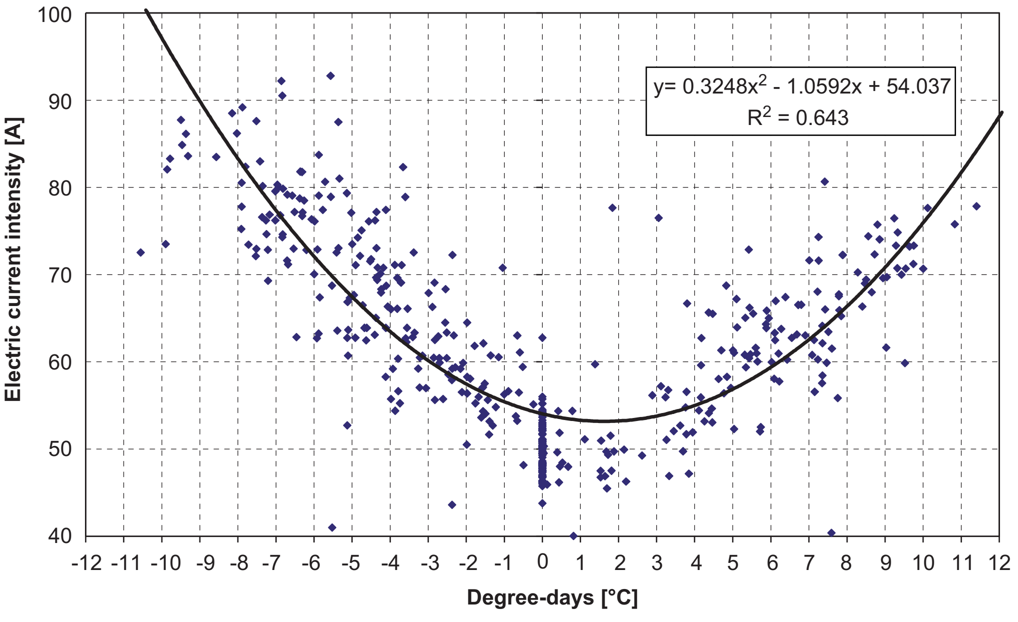


Fig. 6. Relationship between daily mean electric energy intensity and degree-days for the whole period from 01/06/2002 to 10/09/2003.

temperature of 22 °C. The base temperature chosen for the calculation of HDD was the minimum value (18.7 °C) of the regression curve showed in Fig. 4. The relationship between average daily energy consumption, HDD and CDD is showed in Fig. 6. In Fig. 7 the electricity demand is split into the cooling period and the heating period. In this case the determination coefficient is the same ($R^2 = 0.6$ for the cooling period and $R^2 = 0.7$ for the heating period) whether using a linear or a quadratic regression. An increase of one degree-day in summer is associated with an increase of the daily average current intensity of 3.58 A, whereas the same increase in winter increased energy consumption by 2.26 A.

4.1.1. The Humidex index

In order to estimate the number of AC appliances which are likely to be switched on in the dwellings located within the studied area a thermal discomfort index was used. In fact it is normal to expect that the decision to turn a cooling system on or off is mainly based on a discomfort sensation felt by the population. It is well known that the threshold conditions determining this discomfort sensation should be evaluated on the basis of the combined effect of temperature, thermal radiation, humidity, air speed, clothing insulation and metabolic rate [28]. Furthermore, it is apparent that the use of AC systems is directly influenced by indoor conditions, and only indirectly by the outdoor weather parameters. On the other hand, it has been shown that for the evaluation of the thermal discomfort conditions the same comfort indexes cannot be indifferently used for indoor and outdoor environments, since psychological aspects are important factors, especially outdoors [29].

However, in our case study any information was known about the thermal and hygrometric conditions inside the dwellings, so it was necessary to have resort to a simplified approach, based on the evaluation of the outdoor parameters. In particular, the

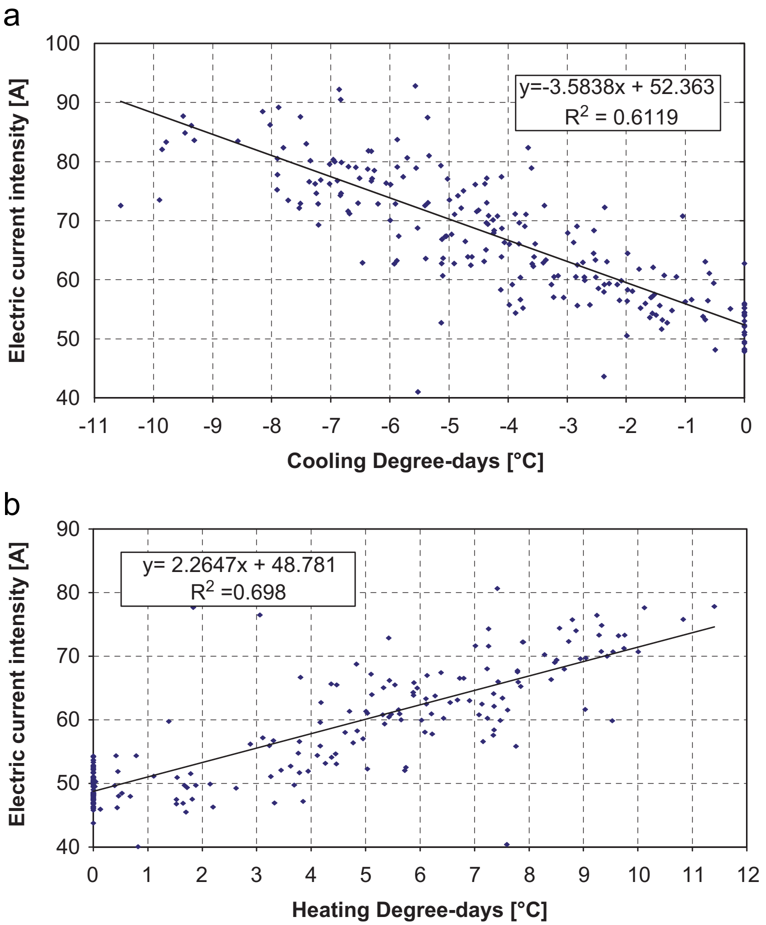


Fig. 7. Relationship between daily mean electric energy intensity and degree-days during: (a) the cooling periods; and (b) the heating periods.

discomfort index called *Humidex index* [30] was used. It is one of the most used discomfort indexes useful to evaluate how current temperature and relative humidity can affect the discomfort sensation and cause health danger for the population. It is defined as follows:

$$H = T + 5/9 \cdot (e - 10), \tag{6}$$

where T is the dry bulb air temperature (in °C) and e is the water vapour pressure of the air (in hPa) measured with a psychrometer. If the value of the water vapour pressure is not available, it can be estimated through a function that combines relative humidity RH and dry bulb temperature T:

$$e = 6.112 \times 10^{[(7.5 \cdot T)/(237.7+T)]} \cdot RH/100. \tag{7}$$

The *Humidex index* expresses in practice an apparent perceived temperature taking into account that an high humidity level in the environment surrounding a human body may obstruct the process of evaporation of the sweat from the human skin. The human body so is not able to eliminate the excessive heat (compared to its own physiological limits)

Table 3
Comfort/discomfort categories related to the values of the *Humidex index*

$H<27$	Full comfort
$27\leqslant H\leqslant 30$	Subtle discomfort
$30' H\leqslant 40$	Great discomfort
$40' H\leqslant 55$	Danger
$H>55$	Imminent heat stroke

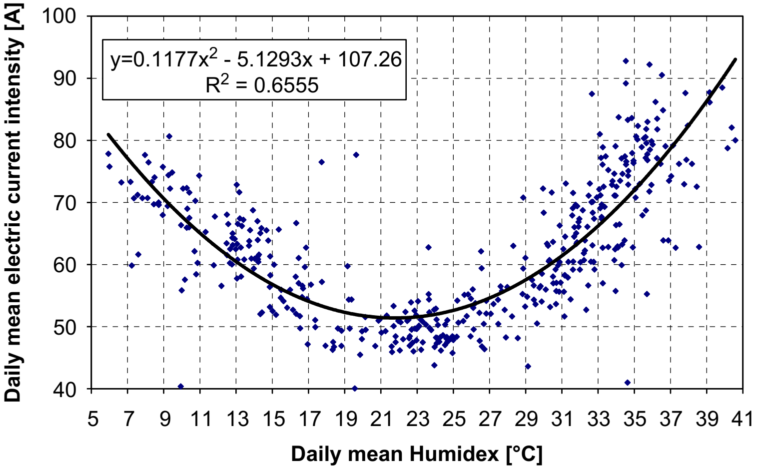


Fig. 8. Relationship between daily mean electric current intensity and *Humidex index* for the whole period from 01/06/2002 to 10/09/2003.

receiving the sensation of an higher temperature. As a consequence, this index is really suitable only for the hot periods, in which the perspiration process is more accentuated.

Some values of H identify different categories of discomfort, corresponding to the levels of alert described in Table 3.

The relationship between the daily mean energy consumption and the daily mean values of *Humidex index* are showed in Fig. 8. In Fig. 9 the electricity demand is split into the cooling period and the heating period. As it is normal to expect, during the winter period almost all the values of the *Humidex index* are lower than 27, corresponding to a "full comfort" situation.

4.1.2. *The HS index*

The technique here adopted for the evaluation of the number of air-conditioners which hour by hour are likely to be switched on, was inspired by the statistical technique known as Probit analysis, which is employed to model the percentage of a sample responding to various levels of exposure to an environmental agent. Probit analysis has been widely used in thermal comfort research [31]. For the present study any information was known about the utilization patterns of the air-conditioners, so it was impossible to perform a Probit regression between values of *Humidex index* and probability of appliances being switched on. For this reason a sigmoidal response function between the two variables was fitted. Its equation was determined so that the probability of an air-conditioner being switched on

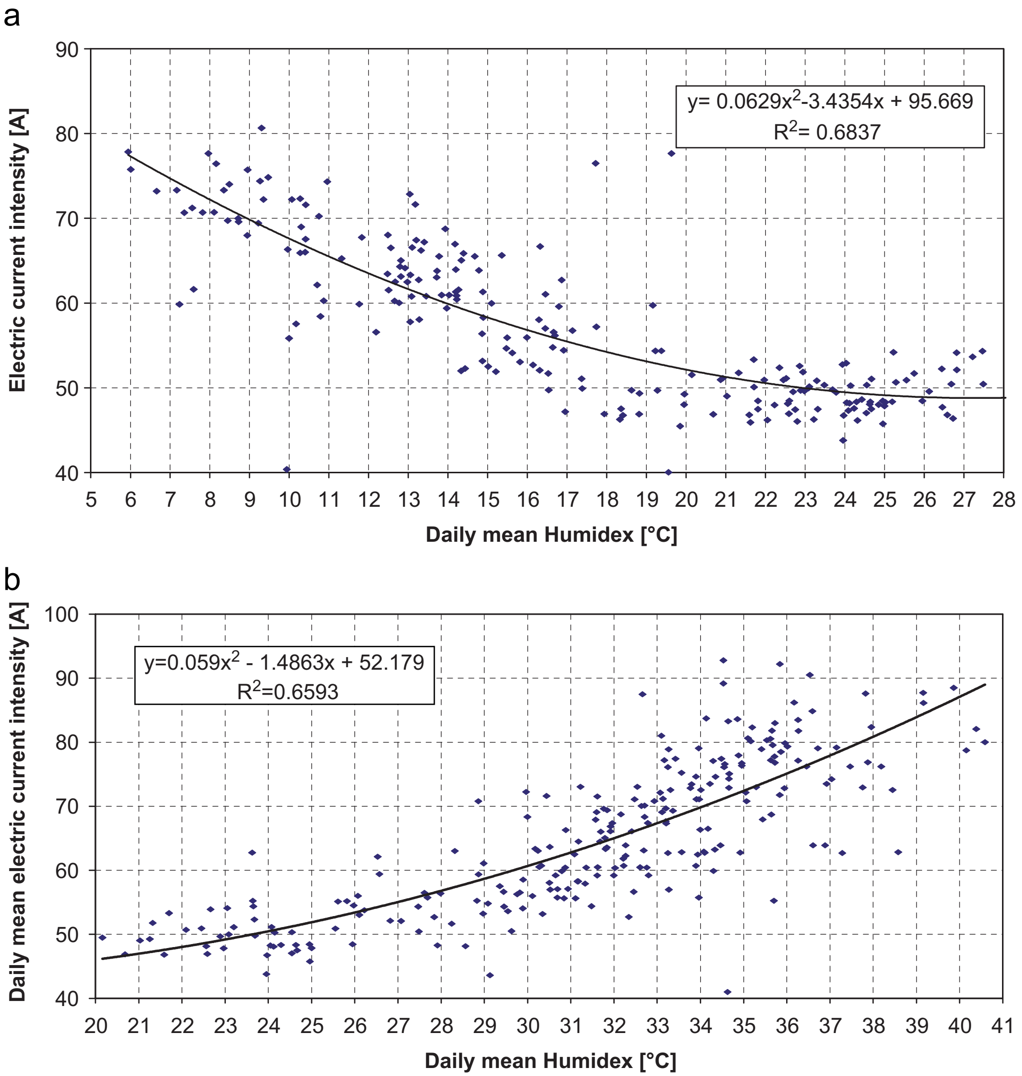


Fig. 9. Relationship between daily mean electric current intensity and *Humidex index* during: (a) the heating periods; and (b) the cooling periods.

was equal to 5% when the value of H was 27 (threshold value between the *subtle discomfort* and the *full comfort* classes in Table 3) and to 95% when the value of H was 55 (value likely to cause the beginning of a *danger* situation as reported in Table 3).

The equation of the sigmoid with these constraints is the following:

$$P_t = \frac{1}{1 + e^{-0.210317\cdot(H_t - 41)}}, \tag{8}$$

where P_t is the proportion of air-conditioners switched on at hour t; H_t is the value of the *Humidex index* at hour t.

The value of the *HS index* at hour t is finally obtained as the product of P_t and the number of air-conditioners determined for the same hour t with the method described in Section 4.1.

4.2. Data pre-processing

The data pre-processing consists in an outliers' elimination procedure, followed by a scaling operation. In order to eliminate the outliers from the data base, the frequency histograms of each variable referred to whole multiples of the standard deviation were plotted.

In Fig. 10 each bar represents the number of times the differences between the values of the variable and their average value was greater than or equal to the whole multiple of the standard deviation indicated in the corresponding tick in the X-axis. By the observation of these histograms, for each variable (except the solar radiation) it was decided to eliminate all the values whose difference from the mean value was greater than the double of the standard deviation. For the solar radiation the threshold value was set to three times the standard deviation.

Afterwards, the described operation was repeated for the values contained into a window of 48 h which was moved along the whole data vector. The first and the last 24 values of each vector were not processed by this second elimination procedure and were not considered as outliers.

The second pre-processing operation consists of a normalization treatment. This operation allows a more rapid convergence and reduces the risk to get stuck in local minima of the error function during training.

All the input data were normalized between an upper and a lower bound. Each sample of data was multiplied by an amplitude term and shifted by an offset term. These two terms were computed by using the following equations:

$$A(i) = \frac{U - L}{\max(i) - \min(i)}, \tag{9}$$

$$O(i) = U - A(i) \cdot \max(i), \tag{10}$$

where $A(i)$ is the amplitude term; $O(i)$ is the offset term; U is the upper bound; L is the lower bound; max(i) and min(i) are the maximum and minimum values for the variable I, respectively.

The linear equation used for the data normalization procedure is the following:

$$x(i)_{\text{norm}} = A(i) \cdot x(i) + O(i), \tag{11}$$

where $x(i)_{\text{norm}}$ is the normalized value of the generic vector component of the variable i; $x(i)$ is the raw value of the same component.

The values of the upper and the lower bound used for all the variables are, respectively, $U = 0.9$ and $L = -0.9$.

4.3. Learning procedure

The learning algorithm utilized for the network's training is the *backpropagation with momentum*, whose adaptive rule for weights updating is given by the following

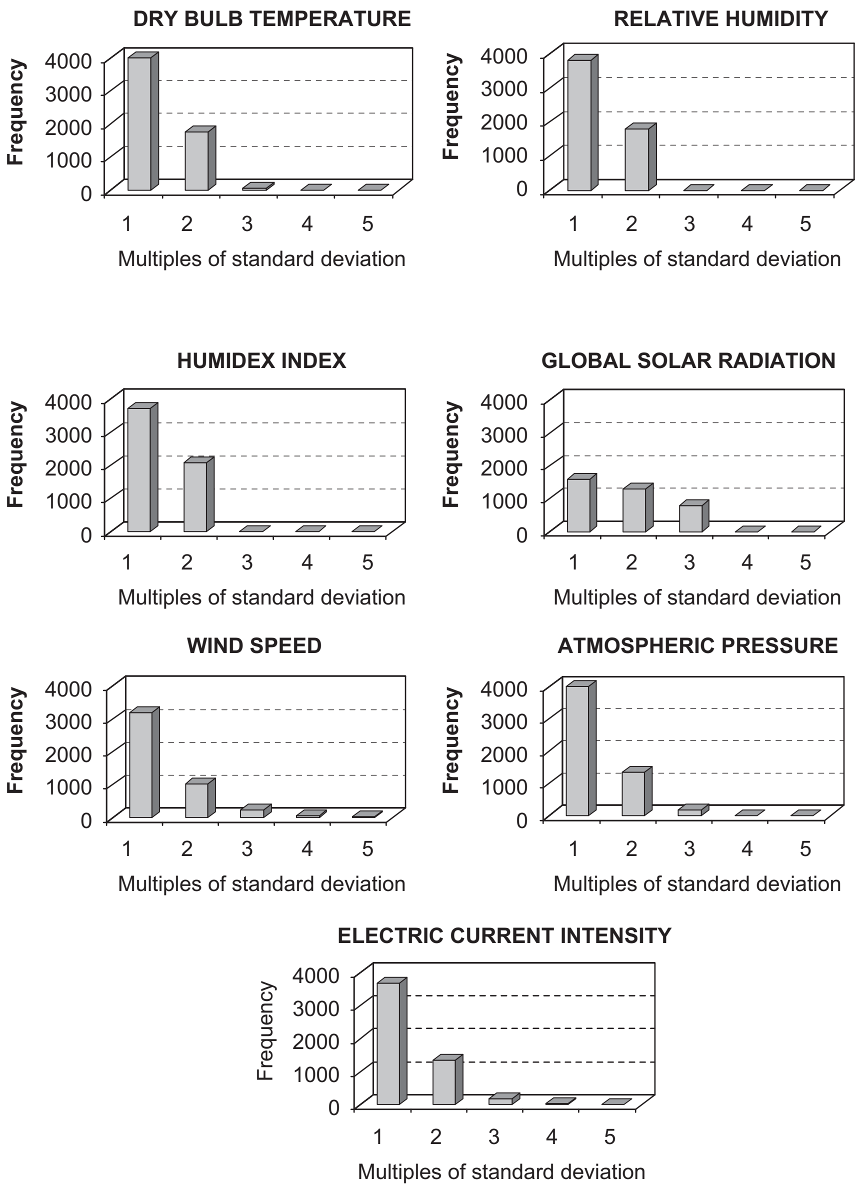


Fig. 10. Frequency histograms for the weather variables. Each bar represents the number of times the difference between a value of the variable and the average value of the same variable was greater than or equal to the whole multiple of the standard deviation indicated in the corresponding tick in the *X*-axis.

equation [32]:

$$w_{ji}(t+1) = w_{ji}(t) - \eta \frac{\partial E}{\partial w_{ji}}(t) + \alpha \Delta w_{ji}(t-1), \tag{12}$$

where $w_{ji}(t+1)$ is the value, at the training step $(t+1)$, of the weight associated with the connection from neuron i to neuron j; $w_{ji}(t)$ is the value of the same weight at the training step t; η is the *learning rate*, a term which reduces the derivative of the error function and has an important effect on the time needed till up convergence is reached; $E(t)$ is the error function to minimize with the training process and its value is related to the difference, at time t, between the output calculated by the network and the desired value at the same time; α is the *momentum* parameter and its effect is the reduction of the influence of the previous step on the current.

If η is too small, the training process requires too many steps to reach an acceptable solution; on the other hand, a large learning rate could lead to oscillations, preventing the error to fall under a fixed threshold value. The additional term α makes the learning procedure more stable and accelerates the convergence process in the shallow regions of the error surface.

Different values of η in the interval $[0.1, 1]$ and α in the interval $[0.5, 0.9]$ were used to train the network and the chosen ones are $\eta = 0.1$ and $\alpha = 0.7$.

4.4. Neural model selection

As previously stated, several different Elman networks were tested varying the number of neurons in the hidden layer, the number of variables used as inputs of the model and the embedding dimension. The contribution of wind speed and atmospheric pressure to the improvement of the forecasting performances of the networks was negligible, so these two variables were not taken into account and further investigations were accomplished only on models based on the following inputs (with an *embedding dimension* $d = 1$):

- $h(t-1)$, the number indicating the hour of the day (from 0 to 23) for the hour $(t-1)$,
- $HS(t-1)$, the value of the *HS index* at hour $(t-1)$,
- $T(t-1)$, the external air dry bulb temperature at hour $(t-1)$,
- $R(t-1)$, the solar total radiation at hour $(t-1)$,
- $C(t-1)$, the electric current intensity at hour $(t-1)$, and
- $H(t-1)$, the value of the *Humidex index* at hour $(t-1)$.

Table 4 shows the results obtained with the main Elman networks tested in comparison with a MLP trained on the same data. The Elman network with 50 hidden units (and 50 context units) gave the best results in terms of absolute percentage error (APE):

$$\mathrm{APE} = 100 \cdot \left| \frac{\hat{y}(t_i) - y(t_i)}{y(t_i)} \right|, \tag{13}$$

Table 4
Summary of structures and performances of the neural networks tested

	Elman				MLP
	25 neurons	50 neurons	75 neurons	100 neurons	50 neurons
Maximum APE (%)	18.3	10.9	17.5	17.1	51.6
Average APE (%)	6.2	3.1	6.1	6.6	5.4
Variance of APE	21.1	6.9	23.2	25.3	37.1

where $\hat{y}(t_i)$ indicates the forecasted current intensity at hour t_i and $y(t_i)$ indicates the observed current intensity at the same hour.

The activation function of the neurons of the hidden and the output layer is the hyperbolic tangent sigmoid function, which is described by the following equation:

$$f(x) = \tanh(x) = \frac{1 - e^{-2x}}{1 + e^{-2x}}. \tag{14}$$

The generic ith neuron of the context layer integrates with a time constant r_i the activity received by the corresponding neuron in the hidden layer. This operation implements a normalized feedback from the scaled output of the hidden neurons to their input. The output of the ith context neuron at time t is expressed by the following equation:

$$k_i(t) = z_i(t) + r_i \cdot k_i(t-1), \tag{15}$$

where $z_i(t)$ is the output of the corresponding ith hidden neuron at time t; $k_i(t)$ is the output of the ith context neuron at time t and r_i is its *recency constant* mentioned in Section 3. It is possible to use a different recency constant for each of the hidden neurons.

In the Elman network presented in this paper the recency constant of each context neuron was set equal to 0.8. Only 10,170 samples of the available data set were used as cross validation set, 168 samples (the week from 17/07/02 to 23/07/02) were used for the *recall phase*, i.e. to test the networks forecasting performances after training, and the remaining 9200 data constituted the training set. The early stopping criterion was implemented in order to prevent overfitting. The generalization ability of the network was evaluated on the basis of the APE.

The actual and forecasted values of the electric current intensity for the chosen week are plotted in Fig. 11, along with the corresponding values of APE.

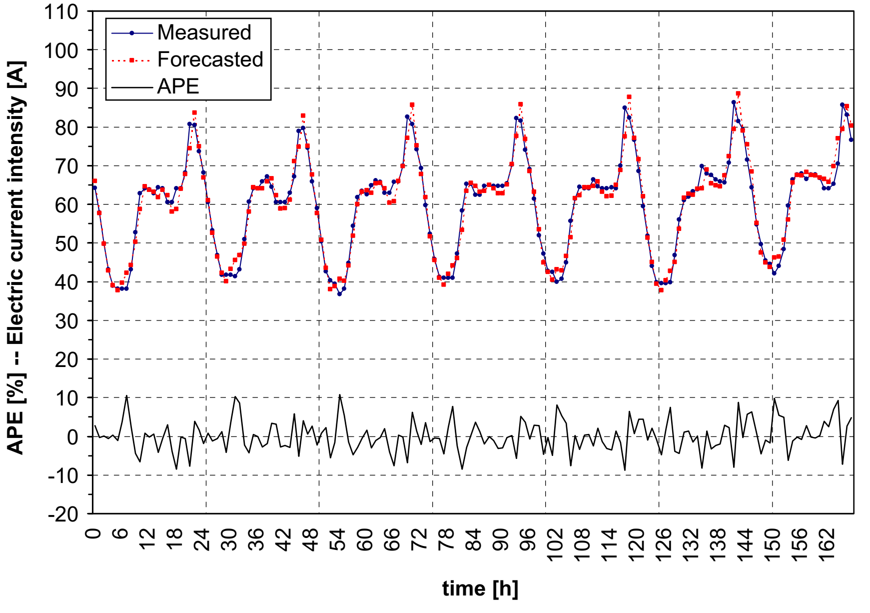


Fig. 11. Performances of the model for the week 17/07/02–23/07/02.

5. Sensitivity analysis

The appraisal of the effects that each of the network inputs is having on the network outputs is an important element for improving the knowledge of the internal representations generated by a NN. This provides feedback as to the saliency of the input variables, so leading to a better understanding of the studied phenomenon. From this analysis, one may decide to prune the input space by removing the insignificant channels. This will reduce the size of the network, which in turn reduces the complexity and the training times.

In ANN research not much attention has been paid to this aspect. Without a sensitivity analysis it is not possible to immediately find out how the weights of the network or the activation values of the hidden neurons are related to the set of training data. Thus, unlike classic statistical models, in a NN the effect that each input variable has on the dependent variables is not made explicit.

Sensitivity analysis is based on the measurement of the effect that is observed in the output y_k due to the change that is produced in the input x_i. Thus, the greater the effect observed in the output, the greater the sensitivity with respect to the input. Obtaining the Jacobian matrix by the calculation of the partial derivatives of the output y_k with respect to the input x_i, that is $\partial y_k/\partial x_i$, constitutes the analytical version of sensitivity analysis.

In this paper the assessment of the relative importance of the input variables was accomplished through a *numerical sensitivity analysis* (NSA) technique [33].

In order to use the NSA method the patterns were first arranged in ascending order according to the values of the input variable x_i. As suggested by Montaño and Palmer [33], a number $G = 30$ of groups of equal, or approximately equal, size was generated for each variable, except for the variable h, for which the number of the groups generated is 24, how is suggested by the nature of the variable itself.

For each group g_r formed, the correspondent output was then computed by the trained network and the arithmetic mean of the variable x_i and of the variable y_k were calculated. Then the NSA index was obtained based on the numeric calculation of the slope formed between each pair of consecutive groups g_r and g_{r+1}, of x_i over y_k through the expression:

$$\mathrm{NSA}_{ik}(g_r) = \frac{\bar{y}_k(g_{r+1}) - \bar{y}_k(g_r)}{\bar{x}_i(g_{r+1}) - \bar{x}_i(g_r)}, \tag{16}$$

where $\bar{x}_i(g_r)$ and $\bar{x}_i(g_{r+1})$ are the average values of the variable x_i corresponding to the groups g_r and g_{r+1}, respectively, and $\bar{y}_k(g_r)$ and $\bar{y}_k(g_{r+1})$ are the average values of the variable y_k corresponding to the groups g_r and g_{r+1}, respectively.

Once the G-1 values of the NSA index had been calculated, the value of the NSA_i index or slope between the input variable x_i and the output variable $y_k$was obtained by applying the expression:

$$\mathrm{NSA}_i = E(\mathrm{NSA}_{ik}(g_r)) = \sum_{r=1}^{G-1} \mathrm{NSA}_{ik}(g_r) f(\mathrm{NSA}_{ik}(g_r)) = \frac{\bar{y}_k(g_G) - \bar{y}_k(g_1)}{\bar{x}_i(g_G) - \bar{x}_i(g_1)}, \tag{17}$$

where $f(\mathrm{NSA}_{ik}(g_r)) = [\bar{x}_i(g_{r+1}) - \bar{x}_i(g_r)]/[\bar{x}_i(g_G) - \bar{x}_i(g_1)]$ represents the probability function of the NSA index; $\bar{x}_i(g_G)$ and $\bar{x}_i(g_1)$ are the average values of the variable x_i for the last group g_G and the first group g_1, respectively; $\bar{y}_k(g_G)$ and $\bar{y}_k(g_1)$ are the average values of the variable y_k for the group g_G and the group g_1, respectively.

Table 5
Values of NSA index and relative standard deviation (SD) for each of the input variables of the trained neural network

Variable	NSA_i	SD of NSA_i
HS index	0.23	12.44*
Hour	0.11	0.70
Humidex index	0.21	0.76
Electric current intensity	0.55	0.36
Global solar radiation	−0.06	0.3
Dry bulb temperature	0.22	1.19

*Value of the SD of the NSA index computed with all the groups. The SD computed only with the first 15 groups is 15.68, with the groups from 16 to 30 is 0.62.

In the model described in this paper there is only one output variable, therefore in Eqs. (16) and (17) it is always $y_k = C(t)$, i.e. the forecasted electric current intensity at time t.

In the application of this sensitivity analysis method all the input and output variables were re-scaled to the same range (between 0 and 1) in order to avoid possible biases in obtaining the NSA index, due to the use of different measurement scales between the input variables.

The higher is the value of the NSA index obtained for an input variable, the bigger is the effect of that variable on the output of the network. A positive value of the NSA index indicates a positive relation between input and output. The values near or equal to zero indicate the absence of effect of the input variable.

The value of the standard deviation of the NSA index was also calculated for the generic input variable x_i. It should be interpreted as the quantity of oscillations that the slope has undergone: the greater the value of the standard deviation, the more chaotic or random the behaviour of the function between the two variables. The values of the NSA index obtained for each of the input variables of the trained NN are showed in Table 5, along with the values of the standard deviation. As it was normal to expect, the highest influence on $C(t)$ is due to $C(t-1)$; it is followed by the *HS index*, the *Humidex index* and the air temperature. The negative value of the NSA index related to global solar radiation is probably due to the rise in electric energy use for lighting during the night, when solar radiation is null.

For a better understanding of the underlying function between the input variable and the output variable, in Figs. 12–17 it is showed a graphic representation of the slope between the input-output couples for the variables with the highest sensitivities ($C(t-1)$ excluded). For each of these variables the evolution of the NSA index computed between each pair of consecutive groups is also showed. Fig. 12 shows the relationship between the *HS index* and the network output. It is apparent that there is a number of air-conditioners (about 9, the average value of the group 14) above which the electric demand starts to rise.

By plotting (Fig. 13) the values of the NSA indexes obtained for each pair of groups, it is possible to observe that the NSA index has an unstable trend up to the group 15 (namely the value of the NSA index computed between groups 14 and 15).

This is testified by the high value of the standard deviation (SD = 15.68) obtained by considering the first 15 groups, compared with the value obtained taking into account the remaining groups (SD = 0.62). From the group 15 on, the behaviour of the NSA index for

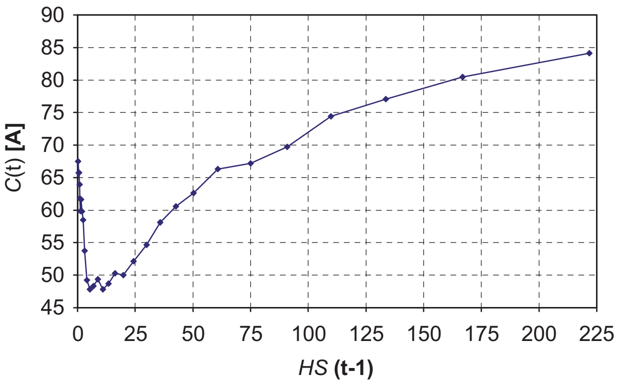


Fig. 12. Graphic representation of the relationship between the *HS index* and the networks output $C(t)$. The average value of *HS* in each of the 30 groups formed by grouping the input patterns according to the values of *HS* is plotted vs the average value of the corresponding groups containing the outputs of the network.

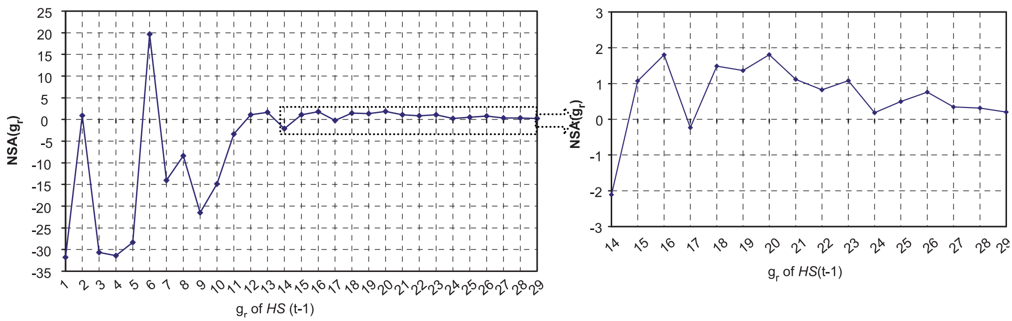


Fig. 13. Graphic representation of the numeric sensitivity analysis applied to the *HS index*. For each group it is plotted the slope (i.e. the value of the NSA *index*) formed between it and its subsequent. On the right side it is showed a detail of the last part of the diagram.

the variable *HS* has a much smaller fluctuation, similar to those of the other significant variables (see Figs. 15 and 17).

It is also important to observe, in the graphic depicted in Fig. 14, that above a value of the *Humidex index* close to 27, correspondent to the beginning of the discomfort class (see Table 3), electric energy demand starts to rise.

6. Conclusions

In this paper a forecasting model based on an Elman ANN trained with the *backpropagation with momentum* algorithm is presented. The model was designed to predict, one hour ahead, the intensity of the electric current supplied to a sub-urban area of the town of Palermo (Italy), characterized by the sole presence of household users. Among the input variables of the model there are both weather data and electric intensity data. The forecasting performances of the network were tested by comparing the model

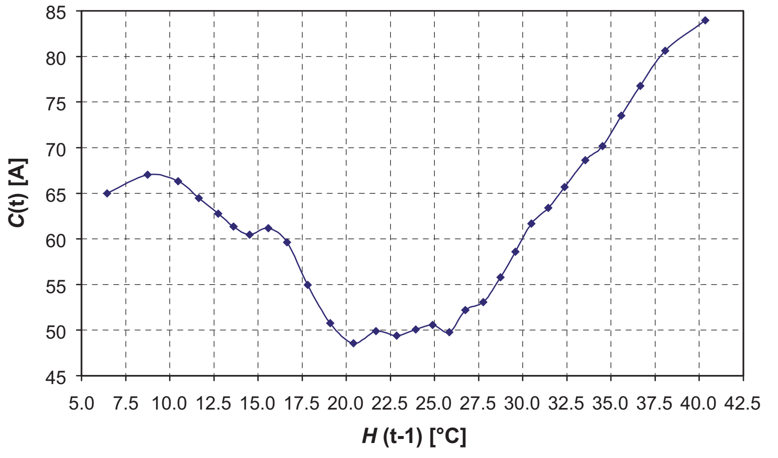


Fig. 14. Graphic representation of the relationship between $H(t-1)$ and $C(t)$. The average value of H in each of the 30 groups formed by grouping the input patterns according to the values of H is plotted vs the average value of the corresponding groups containing the outputs of the network.

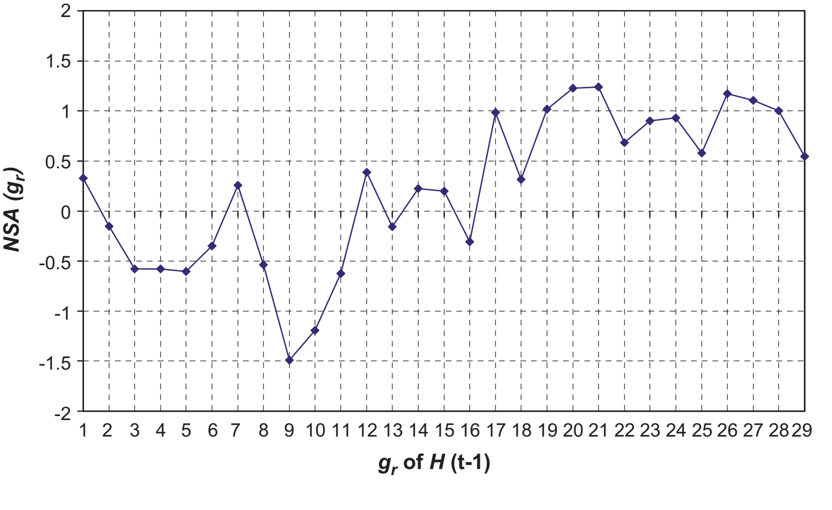


Fig. 15. Graphic representation of the numeric sensitivity analysis applied to the *Humidex index*. For each group it is plotted the slope (i.e. the value of the NSA *index*) formed between it and its subsequent.

predictions with the electric current intensity recorded during a summer week which had never been presented to the network. The average value of the APE obtained for the aforementioned week is equal to 3.1%, with a low variance during the 168 hours of the week.

The work pointed out the importance of a comfort index (*Humidex index*) for the evaluation of the household electricity consumption, underlining how the overall domestic electricity demand is influenced by the use of HVAC appliances. This finding was confirmed by the high sensitivity index (comparable to the one computed for the *Humidex index* and air dry bulb temperature) determined for the *HS index*, a variable related both to

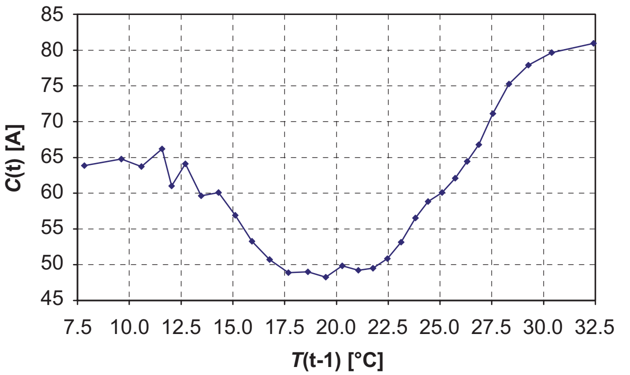


Fig. 16. Graphic representation of the relationship between $T(t-1)$ and $C(t)$. The average value of T in each of the 30 groups formed by grouping the input patterns according to the value of T is plotted vs the average value of the corresponding groups containing the outputs of the network.

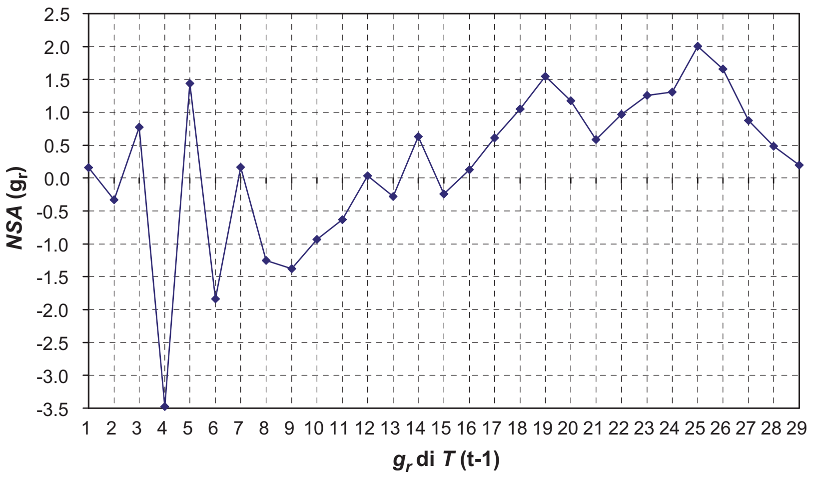


Fig. 17. Graphic representation of the numeric sensitivity analysis applied to the values of T. For each group it is plotted the slope (i.e. the value of the NSA index) formed between it and its subsequent.

the estimated presence of occupants in the dwellings located within the studied area and to the number of AC split systems supposed to be turned on in the same area (see Table 5, NSA_i). In particular, the accomplished analysis pointed out that there is a "critical" number of air-conditioners from which on a raising effect on the electricity consumption starts to be apparent. If the number of air-conditioners that are switched on does not exceed this "critical" value, the effect of the other variables prevails on the use of cooling appliances so that any relevant increase (even a decrease) in electric current demand is recorded. The study represents an example of evaluation of the weather sensitivity of AC appliances in absence of an energy survey about specific end-use electricity consumption, appliance holdings, household characteristics and economic variables. Without these pieces of information it was not possible to apply any of the more

traditional models (e.g. CDA, engineering models) generally used for energy demand estimations in the building sector. Therefore, the choice of a NN model is suitable because of NNs robustness and their capability to maintain satisfactory performances also with noisy and incomplete data as the ones used in our case study.

The work pointed out that, when the parameters generally used to evaluate the indoor comfort conditions (indoor walls and air temperature, vapour pressure in the air, air speed, thermal resistance of clothing, and metabolic rate) are not known, a simple thermal discomfort index like the Humidex (computed using the values of the outdoor air temperature and humidity) is suitable for the explanation of the relationship between climatic conditions and thermal comfort needs of the urban population.

References

[1] Sailor DJ, Pavlova A. Air-conditioning market saturation and long term response of residential cooling energy demand to climate change. Energy Int J 2001;28(9):941–51.
[2] Lopes C, Adnot J, Santamouris M, Klitsikas N. Alvarez S, Sanchez F. Managing the growth of the demand for cooling in urban areas and mitigating the urban heat island effect. Proceedings of ECEEE congress, vol. II, Mandelieu, 11–16 June 2001.
[3] Elman JL. Finding structure in time. Cognitive Sci 1990;14:179–211.
[4] Bartels R, Fiebig DG. Residential end-use electricity demand: results from a designed experiment. Energy J 2000;21:51–81.
[5] Karlsson N, Dellgran P, Klingander B, Garling T. Household consumption: influences of aspiration level, social comparison, and money management. J Econ Psychol 2004;25(6):753–69.
[6] Pedersen L. Use of different methodologies for thermal load and energy estimations in buildings including meteorological and sociological input parameters. Renew Sustain Energy Rev 2007;11:998–1007.
[7] Hart M, de Dear R. Weather sensitivity in household appliance energy end-use. Energy Build 2004;36:161–74.
[8] Larsen BM, Nesbakken R. Household electricity end-use consumption: results from econometric and engineering models. Energy Econ 2004;26(2):179–200.
[9] Aydinalp M, Ugursal VI, Fung AS. Modeling of residential energy consumption at the national level. Int J Energy Res 2003;27:441–53.
[10] Michalik G, Khan ME, Bonwick WJ, Mielczarski W. Structural modeling of energy demands in the residential sector: 1. Development of structural models. Energy 1997;22:937–47.
[11] Tzafestas S, Tzafestas E. Computational intelligence techniques for short-term electric load forecasting. J Intell Robotic Systems 2001;31(1):7–68.
[12] Bartels R, Fiebig DG. Integrating direct metering and conditional demand analysis for estimating end-use loads. Energy J 1990;11(4):79–97.
[13] Parti M, Parti C. The total and appliance-specific conditional demand for electricity in the household sector. Bell J Econ 1980;11(1):309–21.
[14] Ringwood JV, Bofell D, Murray FT. Forecasting electricity demand on short, medium and long time scales using neural networks. J Intell Robotic Systems 2001;31:129–47.
[15] Beccali M, Cellura M, Lo Brano V, Marvuglia A. Forecasting daily urban electric load profiles using artificial neural networks. Energy Convers Manage 2004;45(18–19):2879–900.
[16] Aydinalp M, Ismet Ugursal V, Fung AS. Modeling of the space and domestic hot-water heating energy-consumption in the residential sector using neural networks. Appl Energy 2004;79(2):159–78.
[17] Kalogirou SA. Artificial neural networks in renewable energy systems applications: a review. Renew Sustain Energy Rev 2001;5(4):373–401.
[18] European Union. Energy & transport in figures, Part 2: Energy Brussels; 2006.
[19] Oke TR, Johnson GT, Steyn DG, Watson ID. Simulation of surface urban heat islands under ‘‘ideal’’ conditions at night: part 2. Diagnosis of causation. Boundary Layer Meteorol 1991;56:339–58.
[20] Papadopoulos AM. The influence of street canyons on the cooling loads of buildings and the performance of air conditioning systems. Energy Build 2001;33:601–7.

[21] Axell M, Karlsson F. Europe heat pumps—status and trends, (IEA Heat Pump Centre), Eighth IEA heat pump conference, Las Vegas, Nevada, USA, May 30–June 2 2005.
[22] Indagine statistica sul mercato dei componenti per impianti di condizionamento dell'aria—Rilevazione annuale sul fatturato risultati anno 2004. CoAer Gr.6, 2005 [in Italian].
[23] Italian National Grid Operator (GRTN), Operation data. Available on-line at: ⟨www.grtn.it⟩, access on September 2005.
[24] Geman S, Bienenstock E, Doursat R. Neural networks and the bias/variance dilemma. Neural Networks 1994;4(1):123–32.
[25] Sarle WS. Stopped training and other remedies for overfitting. Proceedings of the 27th symposium on the interface of computing science and statistic, 1995.
[26] Said SAM. Degree-day base temperature for residential building energy prediction in Saudi Arabia. ASHRAE Trans 1992;98(1):346–53.
[27] Büyükalaca O, Hüsamettin B, Yilmaz T. Analysis of variable-base heating and cooling degree-days for Turkey. Appl Energy 2001;69:269–83.
[28] Fanger PO. Thermal comfort. Copenhagen: McGraw-Hill, Danish Technical Press; 1970.
[29] Höppe P. Different aspects of assessing indoor and outdoor thermal comfort. Energy Build 2002;34:661–5.
[30] Masterton JM, Richardson FA. Humidex, a method of quantifying human discomfort due to excessive heat and humidity, CLI 1-79. Environment Canada, Atmospheric Environment Service, Downsview, Ontario; 1979.
[31] Ballantyne ER, Hill RK, Spencer JW. Probit analysis of thermal sensation assessments. Int J Biometeorol 1977;21:29–43.
[32] Haykin S. Neural networks: a comprehensive foundation. 2nd ed. Upper Saddle River, NJ: Prentice-Hall; 1998.
[33] Montaño JJ, Palmer A. Numeric sensitivity analysis applied to feedforward neural networks. Neural Comput Appl 2003;12:119–25.